

## **Turbulent Prandtl Number in Stably Stratified Atmospheric Boundary Layer: Intercomparison between LES and SHEBA Data**

**Igor N. Esau<sup>1</sup> and Andrey A. Grachev<sup>2</sup>**

<sup>1</sup> Nansen Environmental and Remote Sensing Center / Bjerknes Centre for Climate Research, Thormohlensgate 47, 5006, Bergen, Norway. E-mail: igore@nersc.no

<sup>2</sup> Cooperative Institute for Research in Environmental Sciences, University of Colorado / NOAA Earth System Research Laboratory, Boulder, Colorado, USA E-mail: Andrey.Grachev@noaa.gov

*Submitted: December 4, 2006; revisited version April 16, 2007; published June 5, 2007*

**Abstract.** Turbulence-resolving modelling technique, widely known as large-eddy simulation (LES), becomes a popular tool to investigate environmental turbulence and to aggregate the impact of the turbulent mixing on larger, meteorologically important scales. Although the LES are proved to be useful, the technique still needs careful validation against available data sets. In the research of the stably stratified layers, one of the key questions is relative mixing efficiency for heat, mass and momentum. Turbulence mixing efficiency could be measured by the turbulent Prandtl number,  $Pr$ . It is defined as a ratio of the turbulent eddy viscosity to the turbulent temperature diffusivity. Increase of  $Pr$  with increasing stability, measured through the gradient Richardson number, is observed both in the atmospheric field experiments (e.g. SHEBA data) and the turbulence resolving LES data. At the same time,  $Pr$  is observed to decrease with decay of the turbulence intensity, measured through the flux Richardson number and the non-dimensional height. This fact indicates more significant role of the turbulent heat conductivity in the stably stratified boundary layers, possibly due to momentum loss through irradiation of internal gravity waves, which partially offset the general suppression of the turbulent exchange by strong static stability. One practically important consequence of the more intensive momentum mixing than it would be under constant  $Pr$  is that the surface and the atmosphere always remain dynamically coupled. This coupling prevents the surface cooling to values ( $-80^{\circ}$  C or so) characterizing the surface radiative equilibrium, thus significantly warming the polar climates. Direct observational studies of the mixing efficiency are difficult and generally committed only within a shallow surface layer. Laboratory studies are rarely reach strong stabilities. In these circumstances, homogeneous, high quality LES data covering the entire boundary layer are potentially of great significance to theoretical turbulence research as well as parameterization design. In this paper, we show for the first time that the observed SHEBA and numerical LES data are in good agreement across large span of static stabilities. Despite this fact, important discrepancies remain. The discrepancies have been observed for very weakly and very strongly stratified cases where correspondingly observations or numerical simulations are difficult to achieve.

---

<sup>1</sup>Corresponding Author

## Introduction.

Turbulent Prandtl number is a ratio of turbulent eddy viscosity to the turbulent temperature diffusivity, which could be expressed also as a ratio of the Richardson gradient to the Richardson flux numbers (see Appendix A). It is a measure of the turbulent mixing in the atmosphere, namely, its ability to conduct heat by means of turbulent fluctuations. It is known that the flux Richardson number is limited (for review see Pardyjak et al., 2002; Canuto, 2002; Zilitinkevich et al., 2006a,b). The commonly cited value is  $Ri_f \sim 0.4$ . Since the gradient Richardson number,  $Ri_g$ , could be large indefinitely, Pr is expected to be an increasing function of  $Ri_g$  (Kays, 1994) in a stably stratified planetary boundary layer (SBL). This fact has been corroborated by a number of numerical (Schumann and Gertz, 1995), laboratory (Keller and van Atta, 2000) and field (Yague et al., 2006) studies. Perhaps due to computational limitations and relatively low quality of collected and simulated data, those studies did not include extensive intercomparisons of data derived from essentially different sources. Earlier turbulence-resolving simulations (e.g. Mason and Derbyshire, 1990) were rather imperfect due to several reasons: (i) there were few of them, so the dependence should be derived from self-correlated data at different levels within the same model SBL; (ii) the simulations had too coarse resolution to resolve properly all energetic processes, so the turbulent statistics in the model SBL were seriously harmed; (iii) there were no physically correct closure schemes and numerical algorithms around, so the numerical errors had even larger input into the dependence than it is stated in Appendix A. The LES resolution issue and the earlier LES are discussed in Beare and MacVean (2004).

This study is aimed to investigate whether it is possible to assume a universal functional dependence  $Pr = f(Ri_g)$ . Existence of such dependence would be helpful for both theoretical understanding and practical meteorological modelling. In particular, the latter often rely on empirical stability functions,  $f_M, f_H$ , to determine turbulence diffusivity in meteorological models. It has been shown (e.g. Derbyshire, 1999; King et al., 2001; Cassano et al., 2001) that the model results are rather sensitive to the stability functions and especially to their ratio, which gives another formulation of the same Prandtl number. This problem is known as boundary layer decoupling. It has already attracted some attention from both theoreticians (McNider et al., 1995) and field meteorologists (Smedman et al., 1997). One of the reasons is that the decoupling problem is possibly a demonstration of multiple regimes of the atmospheric turbulence in the SBL. This is something similar to multi-regime behaviour found for the turbulent convection (Lorenz, 1963). One practically important consequence is that in reality the surface and the atmosphere remain practically always coupled, thus, preventing the surface temperature to drop to values ( $-80^\circ\text{C}$  or so) characterizing its radiative equilibrium. In the models, however, decoupling is frequently observed. Moreover it is sensitive to the parameterization of the turbulent heat conductivity evolution under radiative cooling as demonstrated in Steeneveld et al. (2006). Since the decoupling has strongly negative impact on quality of meteorological simulations with possible run away blow up of models, it is commonly prevented by *ad hoc*, thus physically ungrounded, increase of turbulent diffusivity. This is clearly demonstrated in a GABLS intercomparison of 20 single-column models by Cuxart et al. (2006). The dependence  $Pr = f(Ri_g)$  will be further compared with a novel theory from Zilitinkevich et al. (2006a).

Another aim of this study is to compare turbulence-resolving simulations (large-eddy simulations or LES) with direct turbulence measurements in the SBL. Comparison of such a technically sensitive parameters as Pr and  $Ri_g$  could reveal physical consistency of the heat

transport between the nature and the LES. As for our knowledge, this intercomparison has not been done yet for a large number of independent LES runs under varying external parameters.

The presentation is organized as following. The next section describes SHEBA, LES and literature data. Section 3 presents the intercomparisons. Section 4 gives the discussion. Section 5 outlines conclusions. Appendix A describes the details and the method of the intercomparison. Appendix B describes some statistical aspects of the procedure.

## 2. SBL data sets.

### 2.1 SHEBA data set

SHEBA is the Surface Heat Budget of the Arctic Ocean project (Uttal et al., 2002). SHEBA has been conducted from a frozen Canadian ice breaker and an instrumentation network placed around it from October 1997 through September 1998 with several periods of intense measurements and related field experiments. SHEBA data at different stages of processing are available for scientific community on-line from <http://sheba.apl.washington.edu/>. The present analysis uses hourly averaged data collected by the instruments at a meteorological mast in “Met City”. The data described in Andreas et al. (1999; 2006) and Persson et al. (2002). The data version used in the study (ASFG3.0) was compiled in January 2001. Fluxes are calculated using the observed, variable surface pressure. As documentation states, both objective and some subjective editing has been done at various stages of the data processing. Hourly averages were calculated as long as at least four 10-minute periods during the hour contained 2 or more minutes of data, which passed the standard quality control routine. The routine also eliminates fluxes observed in the airflow from the ship or through the tower.

The data file we use is **prof\_file\_all6\_ed\_hd.txt**. It contains data from 5 levels, located nominally at 2.2 m, 3.2 m, 5.1 m, 8.9 m and 18.2 m on the 20 m meteorological mast as well as the radiometer and surface data. The sampling levels vary due to the accumulation or melting of snow, so that the 5<sup>th</sup> level was actually at 14 m above the snow surface during the most of the winter. The tower data includes sensible heat and momentum fluxes as well as wind speed and temperature. After some additional selection to respect the numerical stability (see Appendix A), the total data set contained 1052 measurements at the level 2 (at 3.2 m), 4846 at the level 3 (at 5.1 m) and 5091 at the level 4 (8.9 m). The level 1 and level 5 (at 18.2 m) cannot be used in this analysis since the gradients cannot be computed on those levels.

Figure 1 shows distribution of the SHEBA tower data by gradient Richardson number. One important feature to pay attention to is the number of available measurements dramatically decreases for  $Ri_g > 0.25$ , which is often cited as a critical Richardson number. There is practically no reliable data at  $Ri_g > 1 = \lg Ri_g > 0$ , or at least the data quality has to be controlled for every measurement. Figure 2 shows empirical  $Pr = f(Ri_g)$  obtained by averaging of the SHEBA tower data for levels 2 to 4 and plotted against 4 different non-dimensional stability characteristics, namely, the gradient Richardson number, the flux Richardson number, the integral bulk Richardson number and the non-dimensional height of the Monin-Obukhov theory (see the definitions in Appendix A and the description of the data processing in Appendix B). Despite a huge scatter on all plots, the bin averaged mean values express more or less similar empirical dependences across 3 decades of the Richardson number variation. In the interval  $-2 < \lg Ri_g < -0.5$ , where SHEBA has the largest number of measurements, the statistical confidence of

results is high. Thus, accounting for the rather large standard deviations, one can conclude that at all 3 levels, the dependences could be regarded as a single, universal dependence.

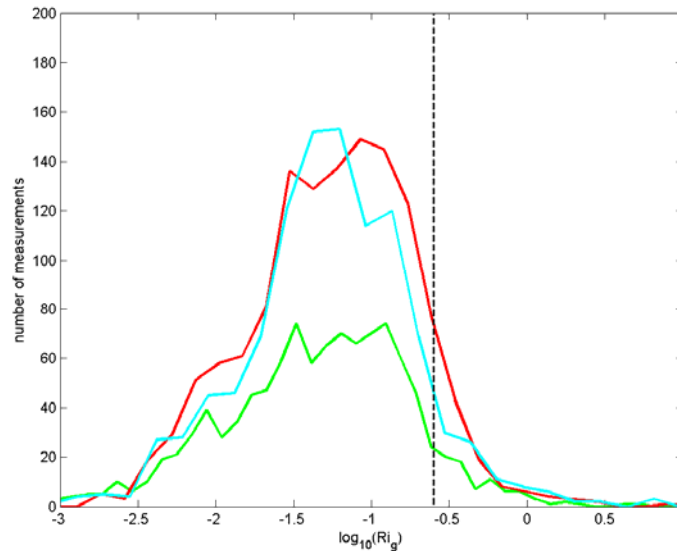


**Figure 1.** Non-normalized distribution of the number of the used SHEBA data by logarithm of the gradient Richardson number: green curve – data at the level 2; red – level 3; cyan – level 4. The dashed line denotes critical Richardson value  $Ri_g = 0.25$ .

It should be noted that SHEBA data implicitly includes effects of radiation flux divergence, ice thermal inertia, the heat leakage under the ice and could be seriously non-stationary as well. Nevertheless, at this stage the SHEBA data may be considered as a “gold” quality standard, something like the “Kansas” for the SBL in terms of duration of the radiative re-stratification, the uniformity of the pack ice surface, the large distance from continent heterogeneities, and often occurrence of slow winds, resulting in the high Richardson number. Andreas et al. (2000) dubbed these conditions as an ideal meteorological “laboratory”. Further analysis of the SHEBA data could be found in recent publications by Grachev et al. (2005), particularly the dependences in question have been presented by Grachev et al. (2003; 2006) during American Meteorological Society and NATO advanced science workshops.

## 2.2 LES data set

Turbulence-resolving simulations have been conducted with the Nansen Centre Large-Eddy Simulation Code LESNIC. The code solves three-dimensional momentum, temperature and continuity equations for incompressible Boussinesq fluid. It employs a fully conservative 2nd order central difference scheme for the skew-symmetric advection term; the 4th order Runge-Kutta scheme for time stepping; and a direct fractional-step pressure correction scheme for the continuity preservation. The computational mesh is the staggered C-type mesh, which demands only fluxes as boundary conditions. The LESNIC employs a dynamic mixed closure, which recalculates the Smagorinsky constant in the eddy diffusivity part of the closure at every time step. Detailed description of the LESNIC was published in Esau (2004), intercomparisons – in Beare et al. (2006) and Fedorovich et al. (2004). The LESNIC has been used to compute a set of

cases, referred to as DATABASE64 (Esau and Zilitinkevich, 2006). In DATABASE64, 80 LES runs are suitable for the present study. All runs have been computed at the equidistant mesh with  $64^3$  grid nodes. The aspect ratio between the vertical and horizontal grid spacing varies from 1:1 to 1:4 with the majority of data computed at the 1:2 mesh. The physical resolution varies from run to run keeping about 25 to 45 vertical levels within the fully developed PBL.

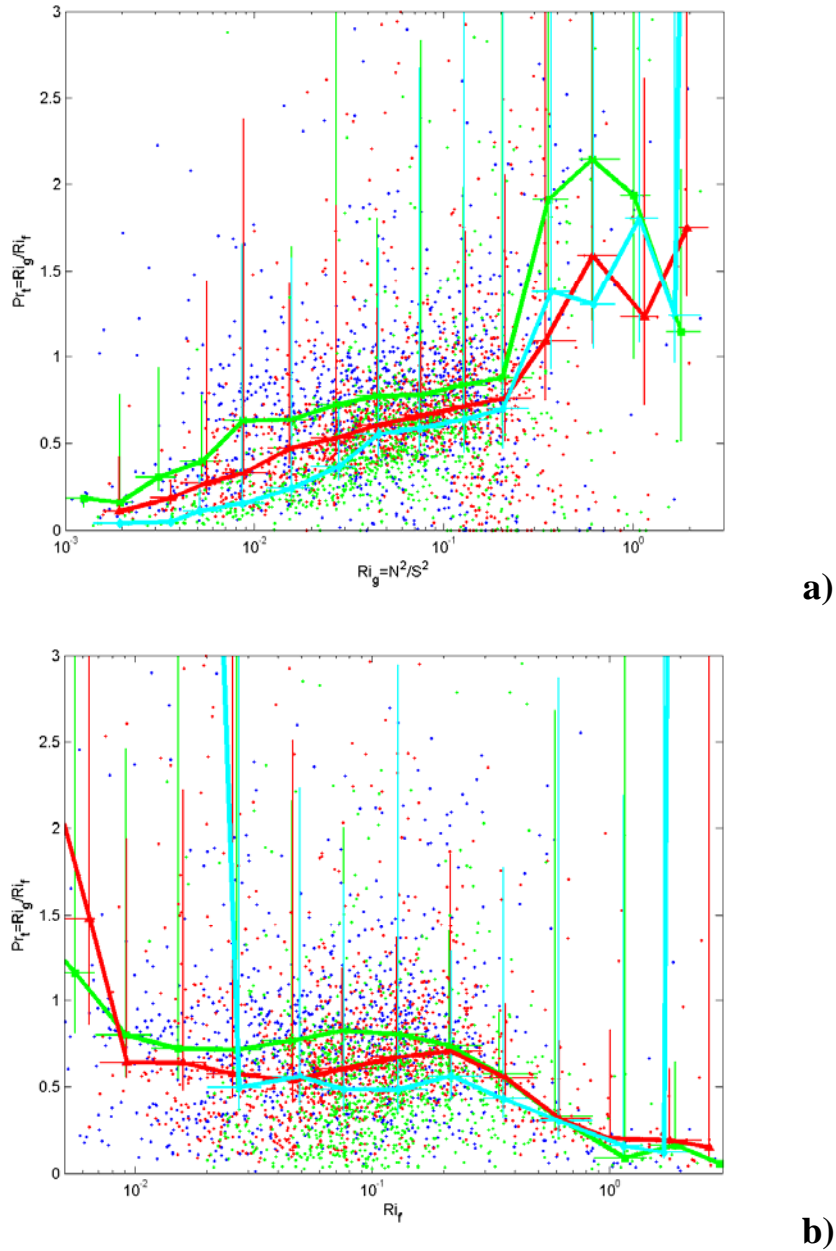
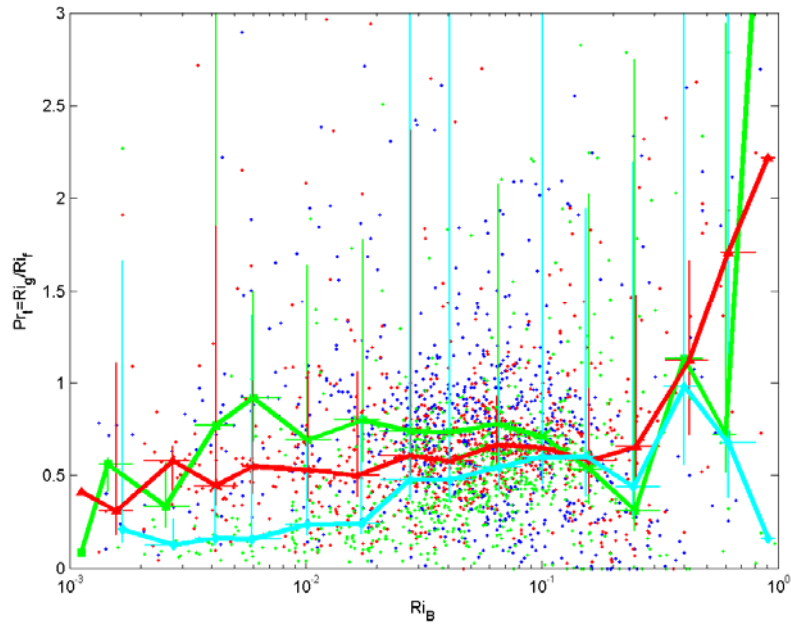
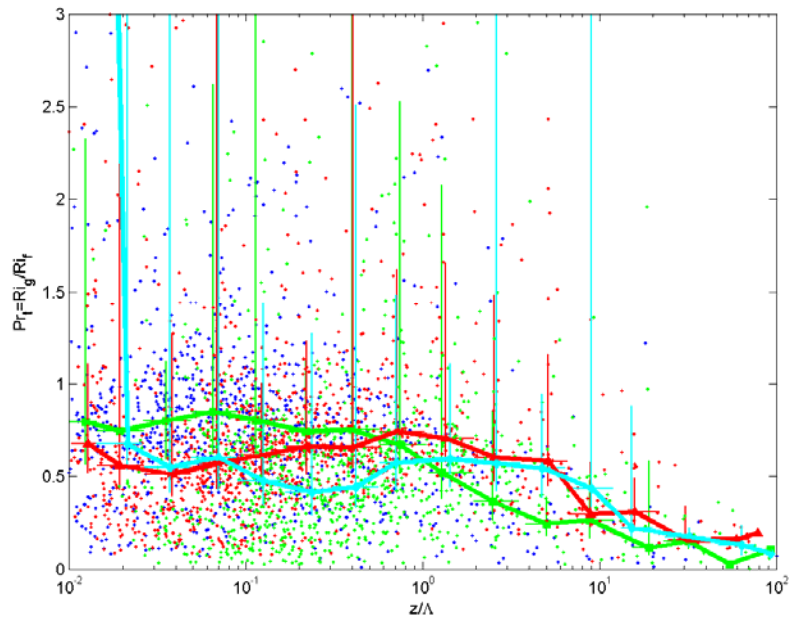


**Figure 2 a and b.** SHEBA data from meteorological mast on turbulent Prandtl number versus different non-dimensional measures of flow static stabilities: (a) gradient Richardson number; (b) flux Richardson number; (see definitions in Appendix A). Green – data at level 2; Red – level 3; Cyan and blue – level 4. Symbols with error bars denote bin averaged values where the horizontal bar denotes the width of the bin and the vertical bar denotes one standard deviation within the bin computed separately for data above and below the average value (see Appendix B). The thick curves identify empirical Prandtl-stability dependences.



c)



d)

**Figure 2 c and d.** SHEBA data from meteorological mast on turbulent Prandtl number versus different non-dimensional measures of flow static stabilities: (c) bulk Richardson number; (d) non-dimensional height (see definitions in Appendix A). Green – data at level 2; Red – level 3; Cyan and blue – level 4. Symbols with error bars denote bin averaged values where the horizontal bar denotes the width of the bin and the vertical bar denotes one standard deviation within the bin computed separately for data above and below the average value (see Appendix B). The thick curves identify empirical Prandtl-stability dependences.

The turbulent boundary layer comprised only 1/2 to 2/3 of the depth of the computational domain. This arrangement assures that the largest eddies, which occupy the entire PBL, were not

affected by the limited horizontal size of the LESNIC domain. The lateral boundary conditions were periodic in all runs. At the surface, the turbulent flux of potential temperature was prescribed and therefore it is considered in this study as an external parameter; whereas the turbulent flux of momentum was computed instantly and pointwise using the log-law. With these boundary conditions, turbulent surface flux parameterizations cannot be evaluated accurately as the surface temperature has not been prescribed in the LESNIC but could be retrieved from the data only with some type of parameterizations. The vertical profiles of the mean variables and the turbulence statistics have been computed from instant resolved-scale fluctuations. All runs in DATABASE64 have been calculated for 16 hours of model time. Only the last hour was used for the time averaging.

The strongest advantage of the LES data in comparison with SHEBA data is that they are available across the entire SBL. This minimises the damping surface effects on the turbulence, which certainly modify the Pr-stability dependences but cannot be regarded as the static stability effect. Another advantage of the LES data is that they are controllable. Possible non-local and diabatic effects are completely excluded. It strongly reduces the data scatter. Nevertheless the scatter remains rather large that could be due to numerical problems with self-correlation and small denominators as well as due to non-monotonic behaviour of numerical schemes. Another possible source for the scatter is turbulence self-organization, which even in the ideal computations will result in formation of certain regions in the flow where non-local effects of the large eddies overcome local dependences.

The strongest disadvantages of the LES data are their dependence on the model resolution, especially under the strongest stratification, and on the surface boundary conditions. This has been demonstrated by Jimenez and Cuxart (2005). Their model based on Deardorff's closure is known to be too dissipative, damping the turbulence near the surface unreasonably. It is also intrinsically prone to run-away cooling due to the pointwise application of the Businger-Dyer universal relationships. This type of surface boundary conditions was tried with LESNIC and found to cause numerical instability as it may not converge to a reasonable flux (Launiainen and Vihma, 1990). Generally, the unnatural run-away cooling in models caused by omission of the radiation processes, which would anchor a radiative equilibrium surface temperature. In result, the LES data were obtained only for relatively strong winds of  $2 \text{ m s}^{-1}$  and larger. Moreover  $Ri_g \gg 0.2$  cannot be sustained in the near surface layer where large Richardson numbers are often observed in SHEBA data. It prompted us to exclude the first 2 model levels from this intercomparison. The resolution dependence is up to some degree alleviated by the choice of the dynamic mixed sub-grid closure. It relates the total kinetic energy of the unresolved sub-grid scale turbulence with the kinetic energy on the smallest resolved scales. Thus, as soon as the model resolve at least a part of the inertial (Kolmogorov or Kolmogorov-Obukhov) interval of scales, the net energy dissipation and thus the net turbulent kinetic energy in the model is maintained approximately correct. Further justification of the robust features of the dynamic closures could be found in Pope (2004). In these conditions, buoyancy suppression of the resolved turbulence causes decay of the net model energy dissipation. At  $Ri_g \rightarrow \infty$  however, a larger portion of the production interval of scales becomes unresolved. Hence, the buoyancy suppression of the resolved turbulence becomes uncorrelated to turbulent kinetic energy on unresolved scales.

### 2.3 Other data sets

Other data involved into this intercomparison are: the extensive data collection prepared by Esau for Zilitinkevich at al. (2006c) report at the Boundary Layer Advanced Workshop in Dubrovnik; and 7 wind tunnel experiments with stably stratified wind tunnel boundary layers described in Ohya (2001). The last two data sets were obtained by personal contact and processed by the first author following the procedure in Appendix A and B in order to comply with conditions of this study.

### 3. Intercomparison

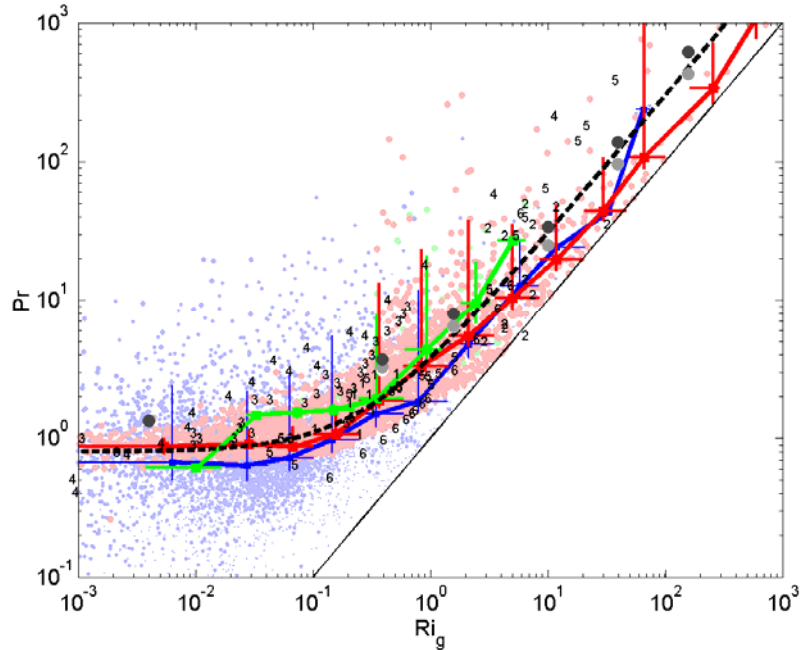


**Figure 3.** Empirical dependence between Prandtl number and Richardson number compiled from different data sources: red dots and curve – the present LES data from DATABASE64; blue dots and curve – SHEBA data; green dots and curve – Ohya wind tunnel data; dark to light grey dots – DNS at resolution  $128^3$ ,  $64^3$ ,  $32^3$  by Stretch et al. (2001). The numbers represent data from literature as: 1 – Bange and Roth (1999); 2 – COSINUS-2000; 3 – Polyakov (1989); 4 – Rehmann and Koseff (2004); 5 – Strang and Fernando (2001); 6 – Monti et al. (2002). Curves represent the bin-averaged values for the corresponding data sets, while the dots represent instant (hourly averaged) samples. The dashed curve is the theoretical approximation by Eq. (1) with  $c_\infty = 3$ .

In this section we analyse different representations of the dependence between the mixing efficiency,  $Pr$ , and the stability expressed through different non-dimensional measures as  $Ri_g$ ,  $Ri_f$ ,  $Ri_B$  and  $z/L$ . Figure 3 shows that  $Pr = f(Ri_g)$  is rather regular function, which can be considered as a universal function by its shape. Qualitatively, the agreement between LES, SHEBA and Ohya data as well as with DNS data is remarkable, while in some intervals of stability the mean curves may diverge by factor of 2. Data from literature reveals something larger spread, which we are not able to explain here. The imperfection of the universality collapse

in the data are probably due to the fact that the atmospheric, numerical and laboratory data reflect different type of perturbations of the stratified unbounded sheared turbulence flow. The later type of the flow has been theoretically considered to suggest the universal behaviour of the mixing efficiency. Such a flow was simulated by DNS by Stretch et al. (2001) but with too small Reynolds number. Zilitinkevich et al. (2006a) theory predicts the following universal approximation

$$Pr = f(Ri_g) = Pr_0 + c_\infty Ri_g, \tag{1}$$

where constants are determined in theory as  $Pr_0 = 0.8$  and  $c_\infty = 5$ . But the data collapse within their single one-sided standard deviation intervals gives a better fit for  $c_\infty = 3$  shown in Fig. 3. Figure 4 shows the reason for the linear increase of  $Pr$  is indeed a saturation of the flux Richardson number at large  $Ri_g$ . The data sets are however uncertain on the actual value of  $Ri_f$  at very large  $Ri_g$ . DNS seem to give the value between 0.3 and 0.4. LES seem to agree with SHEBA and give the values between 0.4 and 0.5. Ohya and some literature data suggest smaller values between 0.08 and 0.2. The agreement within the factor of 2 seems to be found only for sub-critical stabilities at  $Ri_g < 0.25$ .

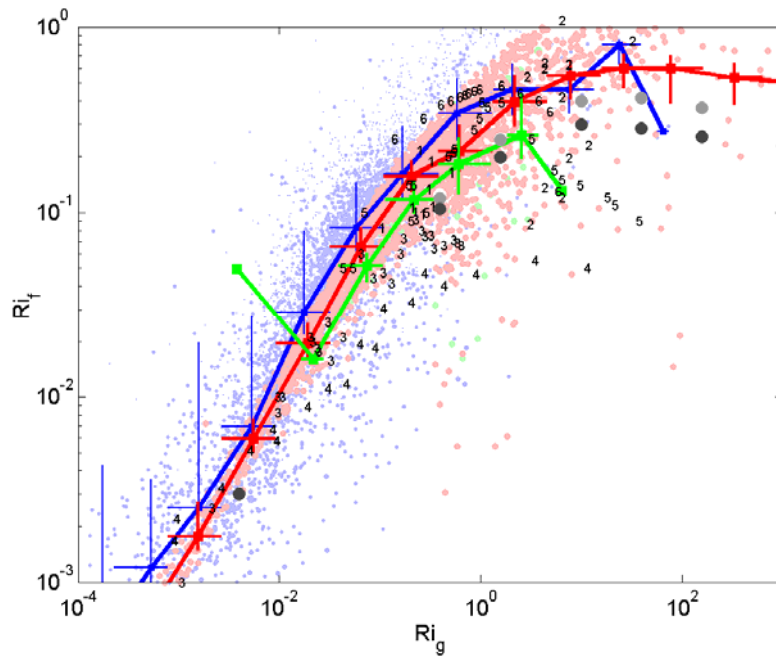


**Figure 4.** Dependence between flux and gradient Richardson numbers. Symbols as in Fig. 3.

So far there were found no significant discrepancies between SHEBA and LES data. This accord breaks when we look at other stability measures. Grachev (2006) has presented and advocated that  $Pr$  is a decreasing function of another popular stability parameter  $z/L$  (see the definition in Appendix A). Contrary, Esau on basis of the experience with LES analysis has suggested that  $Pr$  is an increasing function of  $z/L$ . Figure 5 gives the comparison for SHEBA and LES data. To assure the result, SHEBA data were independently processed by Esau. The dependence corroborates Grachev’s analysis. At the present stage of analysis, we cannot explain the

discrepancy between SHEBA and LES data. Clearly, independent LES studies are needed to assure that this is not a peculiarity of the LESNIC code. Nevertheless, in the area of small  $z/L$ , LES and SHEBA data agree within their standard deviations. At  $z/L > 1$  different tendencies however take place.

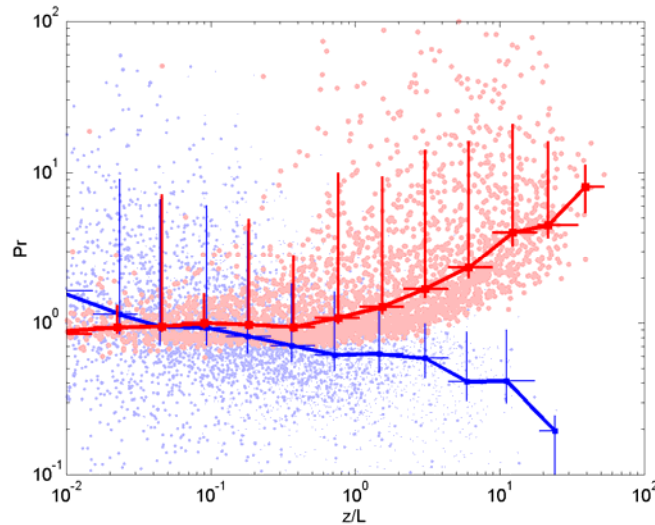


**Figure 5.** Dependence between Pr and the non-dimensional height as a stability parameter  $z/L$ . Symbols as in Fig. 3.

Dependences between Pr and  $Ri_f$ ,  $Ri_B$  are shown in Figures 6 and 7. Figures shows that SHEBA data are much less variable than numerical and wind tunnel data. Since  $Ri_f$  is limited. The Pr dependence should have singularity at critical  $Ri_f$ . It is clearly the case in DNS data at low Reynolds number (usually denoted Re) but the other data sets have considerable number of data, which do not comply. If there is not a data quality issue, the hypothetical explanation may be thought through large eddy structure of the flow. Turbulent flows at high Re are organized in large eddies and existing on their background small-scale turbulence. Those large eddies are asymmetric (Lin, 1997). The larger Re of the flow, the stronger is the asymmetry. Hence a significant portion of data would be sampled in areas where large eddies dominate in the transport of the small-scale turbulence. It causes discrepancy between turbulent fluxes, which are transported from some distant volume and therefore non-local by nature, and the mean gradients, which are local by nature. In such conditions, Pr would be ill-defined as it is computed on the basis of two incomparable quantities, namely, the local gradients and transported fluxes. As atmospheric Re is larger than the effective Re in LES and laboratory, it looks consistent that the large-eddies in the atmosphere are more asymmetric and energetic. This allows for a larger fraction of the non-local flux in data. This non-locality result in nearly constant Pr as function of  $Ri_f$ ,  $Ri_B$ . At  $Ri_f > 0.5$ , SHEBA data in Figure 2b and Figure 6 seem to disagree. Figure 4 suggests that the very existence of such large  $Ri_f$  is questionable. Hence, the disagreement may result from averaging effects on self-correlations, which scatter data in a physically prohibited area of the parameter space. It is worth to mention that on the one hand, the intercomparison with

$Ri_B$  does not have obvious theoretical support. On the other hand,  $Ri_g$  of finite-difference calculations is a kind of  $Ri_b$  but taken over narrow stencil. More accurate higher order numerical schemes require more levels with measurements to compute gradients, and thus increase stencil making  $Ri_g$  even more “bulk”. The calculation technique in Appendix A is just a trade-off for the data available for analysis.

Experience shows one can obtain any kind of  $Pr = f(Ri_g)$  by playing with the layer selection and regularization algorithms. Nevertheless, DATABASE64 data taken over a third of SBL still show increasing  $Pr = f(Ri_g)$  as well as Ohya (2001) data taken over a half of SBL. Unfortunately, there were no direct measurements of the SBL height in SHEBA. It is difficult to estimate the portion of the SBL, which the SHEBA mast covers. Applying the Troen and Mahrt algorithm to the radiosonde data, the mast was not taller than about 10% to 20% of the SBL thickness in the majority of cases. In this shallow layer, SHEBA data do not show certain dependence and could be decreasing or increasing function of  $Ri_B$  depending on interpretation.

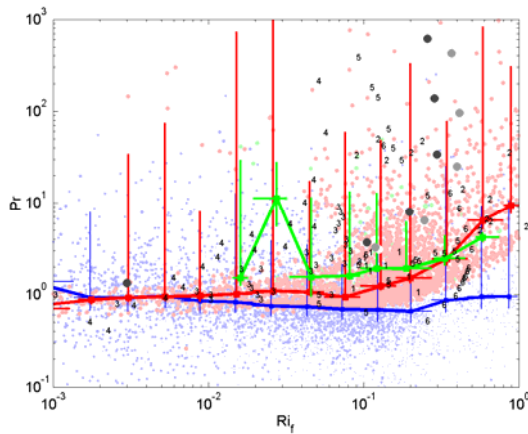


**Figure 6.** Dependence between Prandtl number and the flux Richardson number. Symbols as in Fig. 3.

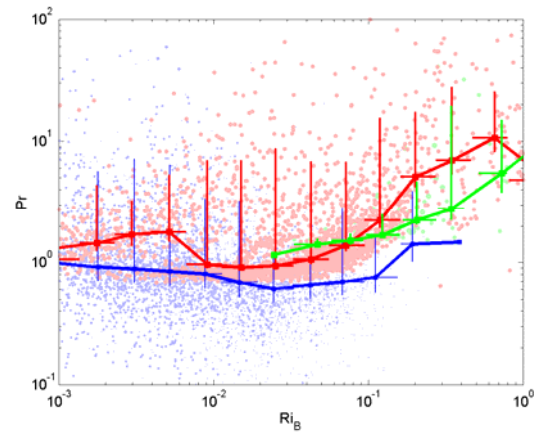


**Figure 7.** Dependence between Prandtl number and the bulk Richardson number. Symbols as in Fig. 3.

## 5. Discussion.

Given the small number, low quality and large scatter of the SBL data at  $Ri_g > 0.25$ , it is not surprising that over 40 years researchers were under illusion of unconditional turbulence decay at super-critical  $Ri_g$ . Our large-eddy simulations provide a fresh look at this problem. Indeed, the turbulence survives well into super-critical regime. The illusion of the total turbulence decay was caused at least in part by the data sampling methods. The sampling methods favour sub-critical sampling, where the fluxes are larger than the instrumental noise. The noise is rather large in cold weather conditions due to number of factors, e.g. icing. Moreover, the sampling within the surface layer is contaminated by an additional damping due to the impenetrable surface proximity. This damping harms mostly the largest and more energetic eddies and force to increase the sampling frequency. Concentration of measurements within the surface layer (10% to 30% of the SBL thickness at best) made the work with strongly stratified layers even more difficult as strong velocity shear within the SBL counter-acts developing of strong stratifications.

Figure 8 from Zilitinkevich and Esau (2006) shows relative scatter in SHEBA and LES data (DATABASE64) plotted for alternative non-dimensional measures of the SBL stability.

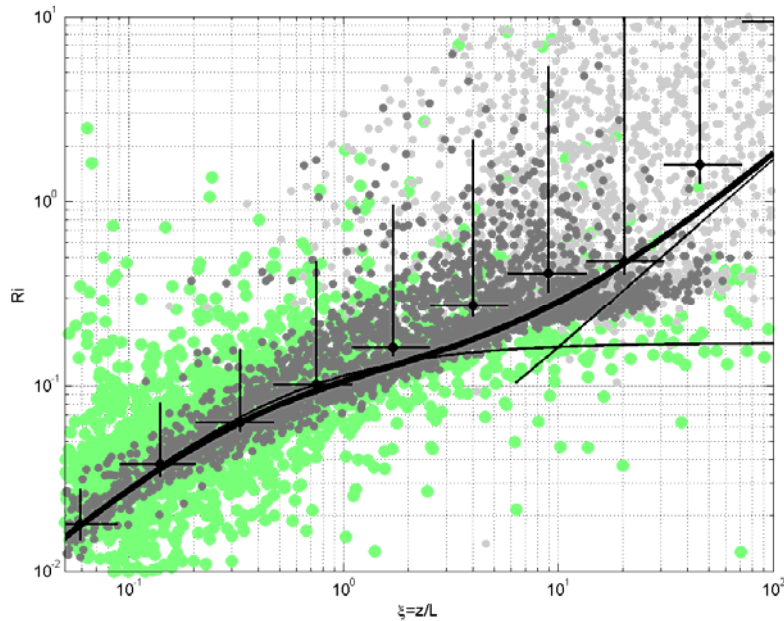


**Figure 8.** Dependence between  $Ri_g$  and the non-dimensional height  $z/L$ : bold line – theoretical curve derived in Zilitinkevich et al. (2006b); thin lines – empirical surface layer (linear) limit and free flow (quadratic) limit; green dots – SHEBA data; dense grey dots – LES data within SBL; light grey dots – LES data above the SBL.

Within the SBL, especially near the surface at weak stabilities, the LES data is much better concentrated than SHEBA data. It helps Zilitinkevich et al. (2006a) and Zilitinkevich and Esau (2006) to develop an instructive theory of the SBL turbulence. The theory relates stability of the flow and the turbulence fluxes with energy exchange between the turbulent kinetic energy – a quantity of wide use in meteorology – and the turbulent potential energy – a quantity introduced in the oceanography (e.g. Strand and Fernando, 2001; Rehmann and Koseff, 2004) and in the fluid dynamics (e.g. Hanadzaki and Hunt, 2004) works but unknown in meteorological applications. This exchange does not modify the sum of those two energies dubbed the turbulent total energy. This fact was proven to be important for further analytical derivations, so that, the analytical curve (bold line in Fig. 5) albeit implicit has been obtained. The curve is surprisingly well matched to the data. This is especially important in the transitional interval between weak stability regime (linear asymptote) and the strong stability regime (quadratic asymptote). This is a demonstration of the theory success as no previous developments were able to approximate analytically this interval.

The idea of the total turbulent energy has already been used for the development of a new parameterization (Mauritzen et al., 2006). Preliminary tests, calibrated on the DATABASE64, have shown a considerable potential of this parameterization. It did improved the single-column model performance versus the GABLS case (Beare et al., 2006), even in a simulation at coarse mesh with resolution close to that in the global meteorological models.

Discussing the data at the strong limit of the stability range, it is worse to remark on the data at the weak limit too. The value of  $Pr_0$  is important for many applications and not less for the meteorological modelling as the near neutral limit is often observed in the atmosphere.  $Pr_0 \sim 0.7$  is thought to be critical as below this threshold a new type of structural instability emerges in the flow. The frequently observed roll-like or streak motions becomes unstable and break down to a more complex pattern as it has been observed in experiments. LES suggest  $Pr_0 = 0.8$  and robust rolls in the flow. Kader and Yaglom (1990) determined even higher  $Pr_0 = 0.95$  in the near-neutral limit of the unstably stratified boundary layer.

As the Figures demonstrate the agreement between data sets becomes worse and the scatter becomes large at small  $Ri_g$ . At the weak stability limit, the LES data seem to be more reliable as they allow calculations of the small gradients with the machine accuracy. Contrary, SHEBA data are rather uncertain as the measurements of small gradients in thin layers are problematic. SHEBA data show systematically smaller  $Pr_0 \sim 0.6$  to  $0.8$  but it is difficult to estimate the exact value. Experimentalists know that in order to obtain small  $Pr_0$ , a mixture of two fluids with strongly different heat conductivities could be used. In the atmosphere this mixture could be air and water vapour or ice/liquid water droplets. Atmosphere in the LES was dry. Hence it is possible that  $Pr_0$  is smaller than  $0.8$ . For comparison, atmospheric SBL data from the VTMX experiment (Monti et al., 2002) do not show such a systematic deviation at weak stabilities. The data from Antarctica (Yague et al., 2001; King, 2006) are uncertain on this issue showing no deviations at the lowermost layers (at about 4 m) but progressively larger deviations at higher layers. Unique to the SHEBA site, the heat is constantly supplied through the sea ice. It could reduce stability while the radiation imbalance added to the turbulence heat diffusion.

## 6. Conclusions.

The proposed format of the DATABASE64 analysis and the LES-SHEBA intercomparison helps to understand mixing efficiency of the stably stratified planetary boundary layers, in particular a practically requested dependence  $Pr = f(Ri_g)$ . The dependence seems to be consistent with the functional form in Eq. (1), while its coefficients remain something uncertain. The analysis allows for a few certain conclusions:

- numerical (DATABASE64 by LESNIC code) and field (SHEBA) datasets are generally in good correspondence to each other when considered against  $Ri_g$
- some difficulties in intercomparison in limits of weak and very strongly static stability remain
- the data sets, analysed against other stability measures than  $Ri_g$ , show only limited correspondents or even contradict each other as in the case of  $z/L$
- the scatter in SHEBA data is large and the data have low statistical significance at super-critical regimes, in contrast, LES data have largely reduced scatter, especially in weakly stable regimes, and any number of LES data could be computed for super-critical regime

## Acknowledgements

This work has been supported by the Norwegian projects NORCLIM 178245/S30, POCAHONTAS 178345/S30, and joint Norwegian-USA project PAACSIZ 178908/S30. Cooperation in frameworks of the NORDPLUS Neighbour 2005-2007 network FI-51 was essential for this study. The authors thank Prof. S. S. Zilitinkevich (Helsinki University) for supporting discussions.

## Appendix A: Method

The non-dimensional flow static stability measures, namely, the gradient, flux and bulk Richardson numbers as well as the non-dimensional height are given by equations below. The equations are defined at the level  $z_n$ .

$$Ri_g = \left( \frac{N}{S} \right)^2 = \frac{g}{\theta_0} \frac{\nabla_z \theta}{|\nabla_z U|^2}, \quad (\text{A.1})$$

$$Ri_f = \frac{g}{\theta_0} \frac{\tau_{\theta 3}}{|\tau_{i3} \nabla_z U|}, \quad (\text{A.2})$$

$$Ri_B = \frac{g z_n (\theta_a(z_n) - \theta_s)}{\theta_0 U(z_n)}, \quad (\text{A.3})$$

$$\frac{z}{\Lambda} = - \frac{|\tau_{i3}|^{3/2}}{\kappa g / \theta_0 \tau_{\theta 3}}, \quad (\text{A.4})$$

Here  $N = \sqrt{\nabla_z \theta g / \theta_0}$  is the Brunt-Vaisala frequency where  $g$  is the gravity acceleration and  $\theta_0 = 300$  K is the reference potential temperature;  $\theta_a(z_n)$ ,  $\theta_s$  are potential temperatures of the air at the height  $z_n$  and the surface temperature. For consistency with LES and laboratory data, where the radiometric temperature of the surface is not defined, the surface temperature here was simply taken as  $\theta_s = \theta_a(z_1)$ ;  $S = |\nabla_z U|$  is the vertical shear of the absolute horizontal velocity component;  $\kappa = 0.41$  (for SHEBA) and 0.47 (for LES) is the von Karman constant. As Eq. (A.1) shows, weak winds and weak vertical wind shears, typical for situations with strong atmospheric static stability, may result in large uncertainties in  $Ri_g$ . This makes the analysis of strongly stratified flows quite difficult. The alternative formulation of the turbulent Prandtl number, which is used in these computations, reads

$$\text{Pr} = Ri_g / Ri_f. \quad (\text{A.5})$$

As follows from Eq. (A.5), Pr is hard to determine when vertical momentum flux  $\tau_{i3}$  or the vertical temperature gradient  $\nabla_z \theta$  are small. These limitations are valid at two opposite ends of the stability range – strong stability with intermittent turbulence,  $Ri_g \rightarrow \infty$ , and weak stability with well mixed potential temperature,  $Ri_g \rightarrow 0$ , correspondingly.

In this study, the data were carefully selected to assure the consistency with the theoretical understanding of processes in fluids. That is, the data with upward fluxes, unstable temperature stratification and the wind speed decreasing with the height have been excluded, in spite of the fact that such conditions could be forced in the atmosphere by non-local effects such as synoptic scale advection, gravity wave propagation and gravity driven currents as well as by diabatic effects such as precipitations, snow saltation, heat leaking from beneath sea ice cracks etc. It does not indicate measurement problems with those data or their relative unimportance but just their inconsistency with idealized understanding of the stable layer turbulent transport in question. To avoid singularities in calculations and to reduce the data scatter, too small denominators leading to Pr and  $Ri_g$  numbers exceeding  $10^4$  have been also omitted.

In addition, the computations are numerically unstable as possible errors for quantities in the denominator could exceed their values. Thus, the resulting Pr and  $Ri_g$  numbers, as well as other non-dimensional characteristics, are sensitive to the accuracy of gradient computations and their correlation with fluxes. We achieve the second order accuracy here by application of the staggered C-type mesh and central difference scheme. The vertical gradients are computed as

$$\nabla_z \varphi(z_n) = \frac{\varphi(z_{n+1}) - \varphi(z_{n-1})}{z_{n+1} - z_{n-1}}, \quad (\text{A.6})$$

where  $\varphi(z_n)$  is any quantity at the height  $z_n$  at the level  $n$  from the surface. To achieve the 2<sup>nd</sup> order accuracy the measurements of fluxes should be organized at the level  $z_n$  between the levels for mean meteorological measurements. Unfortunately this was not the case in field data. Since the measurements of the fluxes and quantities were collocated, the measurements at the bottom and the top levels (levels 1 and 5 in the SHEBA data) cannot be used in computations.

## Appendix B: Statistical processing

As it has been emphasized in Appendix A, the stability measures and Pr are sensitive to the data accuracy. It forced us to limit the data throughout the data processing. In spite of this, a significant number of data result in small gradients and fluxes. In turn, they result in large data scatter, skewed predominantly toward large values of Pr. Thus, in a bin between  $Ri_g - \delta Ri_g$  and  $Ri_g + \delta Ri_g$ , there are number of ill-defined data with very large Pr. As the statistics theory (e.g. Limpert et al., 2001) suggests, a random variable, which is composed by multiplication of many small independent variables and defined on the semi-infinite interval  $[0, \infty]$  like in our case, would be probably distributed log-normally. Figure B.1 supports this view only partially. Indeed the main part of the distribution is approximated with log-linear distribution as

$$f(\text{Pr}, \mu, \sigma) = \frac{\exp\left(-\frac{(\ln(\text{Pr}) - \mu)^2}{2\sigma^2}\right)}{\text{Pr} \sigma \sqrt{2\pi}}, \quad (\text{B.1})$$

where  $\mu, \sigma$  are the mean and the variation of the distribution. Fitting to SHEBA data as in Fig. B.1 gives  $\mu = 0.01, \sigma = 0.35$ . These two parameters allow computations of the geometric mean and median values, which are  $M = \exp(\mu + 0.5\sigma^2) = 1.07, MD = \exp(\mu) = 1.01$

correspondingly. These parameters also give the upper and lower one-standard deviation intervals to be equal to 0.71 and 1.43 correspondingly. The empirical median  $Pr$  for SHEBA within  $0.07 < Ri_g < 0.15$  is 0.78 not 1.01 and the mean  $Pr$  is 1.93 not 1.07.

The difference  $M^{emp} - MD^{emp} = 1.15$  indicates strong skewness of the distribution toward larger values. Thus, the symmetric log-normal distribution is not a satisfactory approximation of the obtained data scatter in a bin. The asymmetry is in part due to data sampling of a strongly increasing function of stability within a finite range of stabilities. The tailed  $Pr$  distribution creates difficulties for interpretation since the regular standard deviation either in the physical or in the logarithmic space cannot be applied. Ridiculous result could be obtained applying the empirical standard deviation 9.98 to the data scattered below the average value since  $Pr$  is a strictly positive definite variable. In these circumstances, we compute one-side standard deviations. That is the standard deviation of the data with  $Pr < MD^{emp}$  and separately with  $Pr > MD^{emp}$ , which reflect the skewed nature of the distribution more accurately.

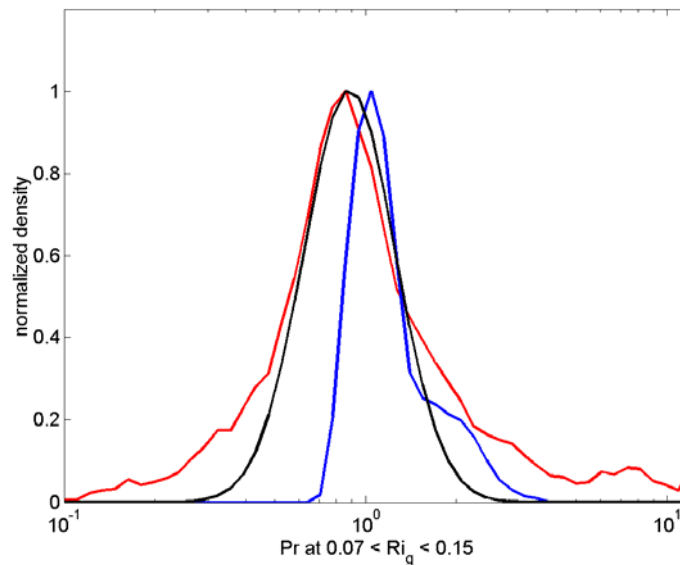


**Figure B.1.** Distribution of  $Pr$  computed for SHEBA (red curve) and LES (blue curve) data in a bin  $0.07 < Ri_g < 0.15$ . The black curve is the best fit of the log-linear distribution in Eq. (B.1) to SHEBA data. See the text for details.

## References

- Andreas, E.L., C. W. Fairall, P. S. Guest, and P. O. G. Persson, 1999: An overview of the SHEBA atmospheric flux program. Preprints, Fifth Conf. on Polar Meteor. And Ocean., Jan. 10-15, 1999, Dallas, TX, 550-555.
- Andreas, E. L., Claffey, K. J., Jordan, R. E., Fairall, C. W., Guest, P. S. Persson, P. O. G., and Grachev, A. A., 2006: Evaluations of the von Kármán Constant in the Atmospheric Surface Layer, *J. Fluid Mech.*, **559**, 117–149.
- Andreas, E.L, K.J. Claffey and A.P. Makshtas, 2000: Low-level atmospheric jets and inversions over the western Weddell Sea. *Boundary-Layer Meteorol.*, **97**, 459-486.
- Bange J., and Roth R., 1999: Helicopter-Borne Flux Measurements in the Nocturnal Boundary Layer Over Land - a Case Study, *Boundary-Layer Meteorol.*, **92**, 295-325
- Beare, R. J., and MacVean, M. K., 2004: Resolution sensitivity and scaling of large-eddy simulations of the stable boundary layer, *Boundary-Layer Meteorol.*, **112**, 257–281

- Beare, R. J., MacVean, M. K., Holtslag, A. A. M., Cuxart, J., Esau, I., Golaz, J. C., Jimenez, M. A., Khairouidinov, M., Kosovic, B., Lewellen, D., Lund, T. S., Lundquist, J. K., McCabe, A., Moene, A. F., Noh, Y., Raasch, S., and Sullivan, P., 2006: An intercomparison of large eddy simulations of the stable boundary layer, *Boundary Layer Meteorol.* **118**, 247 – 272.
- Canuto, V. M., 2002: Critical Richardson numbers and gravity waves, *Astronomy & Astrophysics*, 384, 1119-1123
- Cassano, J. J., Parish, T. R., and King, J. C., 2001: Evaluation of turbulent surface flux parameterizations for the stable surface layer over Halley, Antarctica. *Mon. Wea. Rev.*, **129**, 26–46
- COSINUS Final Scientific Report: Part 2a, 2000: (eds. Berlamont, J. E. & Toorman E. A.), Hydraulics Laboratory, Kong. Univ. Leuven, 68 pp., available at <http://www.hydrumech.uni-hannover.de/cosinus/database/report.html>
- Cuxart, J., and 23 co-authors, 2006: Single-column model intercomparison for a stably stratified atmospheric boundary layer. *Boundary-Layer Meteorol.*, **118**, 273-303.
- Derbyshire, S. H., 1999: Boundary-Layer Decoupling over Cold Surfaces as a Physical Boundary-Instability, *Boundary-Layer Meteorol.*, **90**, 297–325
- Fedorovich, E., Conzemius, R., Esau, I., Chow, F. K., Lewellen, D., Moeng, C.-H., Pino, D., Sullivan, P., and Vila-Guerau de Arellano, J., 2004: Entrainment into sheared convective boundary layers as predicted by different large eddy simulation codes, *16th AMS Symposium on Boundary Layers and Turbulence*, August, Portland, Main, USA
- Esau, I., 2004: Simulation of Ekman boundary layers by large eddy model with dynamic mixed sub-filter closure, *Environmental Fluid Mech.*, **4**, 273-303.
- Esau, I. N., and Zilitinkevich, S. S., 2006: Universal dependences between turbulent and mean flow parameters in stably and neutrally stratified planetary boundary layers. *Nonlin. Processes Geophys.*, **13**, 135–144.
- Grachev, A. A., Fairall, C. W., Persson, P. O. G., Andreas, E. L., Guest, P. S., and Jordan, R. E., 2003: Turbulence Decay in the Stable Arctic Boundary Layer, 7<sup>th</sup> Conference on Polar Meteorology and Oceanography, Hyannis, Massachusetts, AMS Preprint CD-ROM.
- Grachev, A. A., Fairall, C. W., Persson, P. O. G., Andreas, E. L., and Guest, P. S., 2005: Stable Boundary-Layer Scaling Regimes: The SHEBA data, *Boundary-Layer Meteorol.*, **116**(2), 201 – 235.
- Grachev, A. A., E. Andreas, C. Fairall, P. Guest, and O. Persson, 2006: Stable boundary layer over sea ice: the SHEBA results, NATO Advanced Research Workshop on Atmospheric Planetary Boundary Layers, 18-22 April, Dubrovnik, Croatia, available on [http://pbl-nato-arw.dmi.dk/program\\_inc\\_presentations.html](http://pbl-nato-arw.dmi.dk/program_inc_presentations.html)
- Hanazaki, H., and Hunt, J. C. R., 2004: Structure of unsteady stably stratified turbulence with mean shear. *J. Fluid Mech.*, **507**, 1–42.
- Jimenez, M. A., and Cuxart, J., 2005: Large-eddy simulations of the stable boundary layer using the standard Kolmogorov theory: Range of applicability, *Boundary Layer Meteorol.* **115**, 241 – 261
- Kader, B. A., and Yaglom, A. M., 1990: Mean fields and fluctuations moments in unstably stratified turbulent boundary layers, *J. Fluid Mech.*, **212**, 637-662
- Kays, W. M. 1994: Turbulent Prandtl number—where are we? *J. Heat Transfer*, **116**, 284–295
- Keller, K., and Van Atta, C. W., 2000: An experimental investigation of the vertical temperature structure of homogeneous stratified shear turbulence, *J. Fluid Mech.*, **425**, 1-29.
- King, J. C., Connolly, W. M., and Derbyshire, S. H., 2001: Sensitivity of modelled Antarctic climate to surface and boundary layer flux parametrisations, *Quart. J. Roy. Meteorol. Soc.*, **127**, 779–794
- King, J., 2006: Stable boundary layer turbulence: Observations from Antarctica and implications for environmental security, NATO Advanced Research Workshop on Atmospheric Planetary Boundary Layers, 18-22 April, Dubrovnik, Croatia, available on [http://pbl-nato-arw.dmi.dk/program\\_inc\\_presentations.html](http://pbl-nato-arw.dmi.dk/program_inc_presentations.html)
- Launiainen, J. and Vihma, T., 1990: Derivation of turbulent surface fluxes – an iterative flux-profile method allowing arbitrary observing heights, *Eviron. Software*, **5**, 113-124.
- Lin, C.-L., Moeng, C.-H., McWilliams, J. C., Sullivan, P. P., 1997: The effect of surface roughness on flow structures in a neutrally stratified planetary boundary layer flow, *Phys. Fluids*, **9** (11), 3235
- Limpert, B., Stahel, W., and Abbt, M., 2001: Log-normal distributions across the sciences: Keys and clues, *BioScience*, **51** (5), 341–352
- Lorenz, E.N., 1963: Deterministic Nonperiodic Flow, *J. Atmos. Sci.*, **20**(2), 130–141
- Mason, P. J., and Derbyshire, S. H., 1990: Large-eddy simulation of the stably-stratified atmospheric boundary-layer, *Boundary-Layer Meteorol.*, **53**, 117–162
- Mauritsen, T., G. Svensson, S. Zilitinkevich, I. Esau, L. Enger and B. Grisogono, 2006: Energy-similarity – a new turbulence closure model for stably stratified atmospheric boundary layers, *17th Symposium on Boundary Layers and Turbulence*, June 2006, San Diego, California, USA,

- McNider, R. T., Shi, X., Friedman, M., and England, D., 1995: On the predictability of the stable atmospheric boundary layer, *J. Atmos. Sci.*, **52**, 1602-1614
- Monti, P., Fernando, H., Princevac, M., Chan, W. C., Kowalewski, T. A., and Pardyjak, E. R., 2002: Observations of flow and turbulence in the nocturnal boundary layer over a slope, *J. Atmos. Sci.*, **59**, 2513– 2534
- Ohya, Y., 2001: Wind-tunnel study of atmospheric stable boundary layers over a rough surface, *Boundary-Layer Meteorol.*, **98**, 57-82.
- Pardjak, E. R., Monti, P., and Fernando, H. J. S., 2002: Flux Richardson number measurements in stable atmospheric shear flows, *J. Fluid Mech.*, **459**, 307-316
- Persson, P. O. G., Fairall, C. W., Andreas, E. L., Guest, P. S., and Perovich, D. K., 2002: Measurements near the Atmospheric Surface Flux Group Tower at SHEBA: Near-Surface Conditions and Surface Energy Budget, *J. Geophys. Res.*, **107**(C10), 8045, doi: 10.1029/2000JC000705.
- Polyakov, A. Ph., 1989: Single phase mixed convection, *Convective Heat Transfer*, Moklus, 180 pp.
- Pope, S. B., 2004: Ten questions concerning the large-eddy simulation of turbulent flows, *New J. Phys.*, **6**, 35
- Rehmann, C. R., and Koseff, J. R., 2004: Mean potential energy change in stratified grid turbulence *Dynamics of Atmospheres and Oceans*, **37**, 271–294.
- Schumann, U., and Gerz, T., 1995: Turbulent mixing in stably stratified sheared flows. *J. Applied Meteorol.*, **34**, 33-48.
- Smedman, A., Höögström, U., and Bergström, H., 1997: The turbulence regime of a very stable marine airflow with quasi-frictional decoupling, *J. Geophys. Res.*, **102**(C9), 21,049–21,060.
- Steenefeld, G. J., van de Wiel, B. J. H., and Holtslag, A. A. M., 2006: Modelling the arctic stable boundary layer and its coupling to the surface, *Boundary-Layer Meteorol.*, **118**, 357–378
- Strang, E. J., and Fernando, H. J. S., 2001: Vertical mixing and transports through a stratified shear layer. *J. Phys. Oceanogr.*, **31**, 2026-2048.
- Stretch, D. D., Rottman, J. W., Nomura, K. K., and Venayagamoorthy, S. K., 2001: Transient mixing events in stably stratified turbulence, In: 14<sup>th</sup> *Australasian Fluid Mechanics Conference*, Adelaide, Australia, 10-14 Dec 2001.
- Uttal, T., Curry, J. A., McPhee, M. G., Perovich, D. K. and 24 other co-authors, 2002: Surface Heat Budget of the Arctic Ocean, *Bull. American Meteorol. Soc.*, **83**, 255-276
- Yagüe, C., Maqueda, G., and Rees, J. M., 2001: Characteristics of Turbulence in the Lower Atmosphere at Halley IV Station, Antarctica, *Dyn. Atmos. Ocean.*, **34**, 205–223
- Yague, C., Viana, S., Maqueda, G., and Redondo, J. M., 2006: Influence of stability on the flux-profile relationships for wind speed, phi-m, and temperature, phi-h, for the stable atmospheric boundary layer, *Nonlin. Processes Geophys.*, **13**, 185–203
- Zilitinkevich, S. S., T. Elperin, N. Kleeorin, I. Rogachevskii, 2006a: Energy- and flux-budget (EFB) turbulence closure model for stably stratified flows, available on <http://arxiv.org/abs/physics/0610157>
- Zilitinkevich, S. S., Elperin, T., Kleeorin, N., Rogachevskii, I., Esau, I., and Mauritsen, T., 2006b: Turbulent energies and Richardson numbers in stably stratified sheared flows, *NATO ARWorkshop “Atmospheric planetary boundary layers (PBLs): nature, theory and application to environmental modelling and security”*, 17-25 April, Dubrovnik, Croatia, available at <http://pbl-nato-arw.dmi.dk/Presentations/Zilitinkevich.pdf>
- Zilitinkevich, S. S., and Esau, I., N., 2006: Similarity theory and calculation of turbulent fluxes at the surface for the stably stratified atmospheric boundary layers, available on <http://arxiv.org/abs/physics/0612209>